2011-11

Influence of film thickness on the optical transmission through subwavelength single slits in metallic thin films

Applied Optics, Washington, DC : Optical Society of America - OSA, v. 50, n. 31, p. G11-G16, Nov. 2011

http://www.producao.usp.br/handle/BDPI/49721

Influence of film thickness on the optical transmission through subwavelength single slits in metallic thin films

Fabio A. Ferri,[1,*] Victor A. G. Rivera,[1] Sérgio P. A. Osorio,[1] Otávio B. Silva,[1] Antonio R. Zanatta,[1] Ben-Hur V. Borges,[2] John Weiner,[1] and Euclydes Marega, Jr.[1]

[1]Instituto de Física de São Carlos, Universidade de São Paulo, Caixa Postal 369, São Carlos 13560-970, SP, Brazil

[2]Departamento de Engenharia Elétrica, Escola de Engenharia de São Carlos, Universidade de São Paulo, USP, Caixa Postal 359, São Carlos 13566-590, SP, Brazil

*Corresponding author: ferri@ursa.ifsc.usp.br

Received 22 June 2011; revised 1 August 2011; accepted 1 August 2011; posted 3 August 2011 (Doc. ID 149674); published 15 September 2011

Silver and gold films with thicknesses in the range of 120–450 nm were evaporated onto glass substrates. A sequence of slits with widths varying between 70 and 270 nm was milled in the films using a focused gallium ion beam. We have undertaken high-resolution measurements of the optical transmission through the single slits with 488.0 nm (for Ag) and 632.8 nm (for Au) laser sources aligned to the optical axis of a microscope. Based on the present experimental results, it was possible to observe that (1) the slit transmission is notably affected by the film thickness, which presents a damped oscillatory behavior as the thickness is augmented, and (2) the transmission increases linearly with increasing slit width for a fixed film thickness. © 2011 Optical Society of America

OCIS codes: 050.2230, 240.6680, 310.6628, 310.6860.

1. Introduction

Plasmonics is a research field that exploits surface plasmon polariton (SPP) optical excitation of subwavelength-sized structures. Since the spatial localization of these modes is not limited by optical diffraction, it permits the production of small optical elements and potentially new photonic devices [1]. In fact, given that light transmission through small single apertures and periodic arrays is closely related to transmission through waveguides, proper understanding of the relevant physics is critical to new applications such as subwavelength resonant waveguide networks [2].

Ever since the first experimental report on enhanced optical transmission through subwavelength apertures [3], considerable theoretical effort has been devoted to interpreting the essential physics of the process in slit arrays [4–6]. Experimental studies subsequent to the initial report [3] were also performed, which demonstrated a number of surprising features. For instance, spectral transmission measurements [7] revealed that suppression, as well as enhancement, was a characteristic property of slit arrays. Additionally, interferometric studies [8–10] showed that the contribution of transient diffracted surface modes is as important as the SPP guided mode in the immediate vicinity of the subwavelength object. A more recent investigation [11] with the aim to confront the question of how transmission minima and maxima depend on array periodicity showed a minimum in transmission at slit separations equal to the wavelength of the SPP mode, and maxima occurring approximately at half-integer multiples.

However, by focusing attention on the properties of arrays fabricated in metallic films with fixed thickness, these previous studies apparently missed the

0003-6935/11/310G11-06$15.00/0

important role played by the film thickness. For example, in the designing of surface-plasmon-based sensors, a proper choice of the thickness of the metallic film for the optimization of the device sensitivity is very important [12]. There are only a few theoretical [6,12,13] and experimental [14–16] investigations taking into account the influence of film thickness on the considered process. Therefore, the present studies are motivated by the necessity to understand the physics of this phenomenon and to develop optimum designs practices for subwavelength structure fabrication. We present here a systematic study of the optical transmission through subwavelength slits fabricated in Ag and Au film samples possessing different thicknesses. The influence of slit width was also considered. The present work deals with single slits. The extended dimension of the long axis imposes directionality on the transmitted light beam, the divergence of which can easily be controlled [17]. A slit is thus an interesting structure since it combines the compactness of a single defect with the directionality of an array launcher. Moreover, in order to remove measurement ambiguities existing in setups employing an incoherent and broadband light source dispersed through a scanning spectrophotometer [3,7,14–16], we have measured the transmission intensity through the slits using coherent and monochromatic spectral sources [9,11].

2. Experimental Details

A series of silver films with thicknesses of 120, 160, 200, 270, and 330 nm and a set of gold samples with thicknesses of 120, 180, 260, 360, and 450 nm, as measured by a Talystep profilometer, were thermally evaporated onto BK7 glass substrates. Slits with widths in the range of approximately 70–150 nm in the Ag films, and 120–270 nm in the Au films, were milled with an FEI focused ion beam QUANTA 3D 200i (Ga^+ ions, 30 keV). In order to verify the depth of the slits, the gallium ions' source was calibrated using atomic force microscopy. The slit length was fixed at 20 μm. It is worthwhile to remark that 20 μm long slits are suitable for experiments in the optical regime [16,17]. In addition, it is important to mention that the slits fabricated in the Au films are slightly wider than those milled in the Ag samples, probably due to distinct properties between the Au–FIB and Ag–FIB interaction, since the same ion beam conditions were used to fabricate the slits in both Au and Ag films. For example, the right panel of Fig. 1 shows a scanning electron micrograph of a slit with 150 nm of width fabricated in the 200 nm thick Ag film.

We have undertaken a series of high-resolution measurements of the optical transmission through the slits. The transmission measurement setup consists of 488.0 nm (for Ag) and 632.8 nm (for Au) wavelength light beams from Ar ion and HeNe lasers, respectively, with a power of about 1 μW, aligned to the optical axis of a microscope. The beam is focused at normal incidence onto the sample surface by a 20× microscope objective (with an NA of 0.4) in TM polarization (magnetic field component parallel to the long axis of the slits). Light intensity transmitted through each slit is then gathered by an optical fiber and detected with a CCD array detector. It was used on a multimode fiber with an NA of 0.22 and a core diameter of 200 μm. Light intensity is obtained by integrating the signal over the entire region of interest in the CCD image and subtracting the background originating from electronic noise. The transmitted intensity of every slit was recorded in the far-field by the CCD as the sample was stepped using an X-Y translation stage. The left panel of Fig. 1 shows the schematic of the measurement setup.

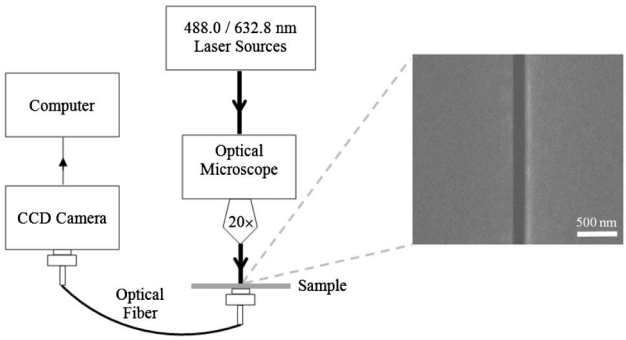

Fig. 1. Left panel shows a schematic of the optical transmission experiment. 488.0 nm (for Ag) and 632.8 nm (for Au) Ar ion and HeNe laser light sources, respectively, are normally focused onto the sample surface by a 20× microscope objective lens. A CCD camera records the transmission intensity through the slits as the sample surface was stepped. Right panel shows a scanning electron micrograph (taken with 40000× magnification) of a typical structure. The considered slit has approximately 150 nm of width and was focused-ion-beam milled through a 200 nm thick Ag layer. In the experiments, the thicknesses of the Ag and Au films were varied in the range of 100–450 nm. The slit length was fixed at 20 μm, and the width is varied from 70 to 270 nm.

3. Results and Discussion

Figure 2 shows the physical picture adopted in this work to investigate the light transmission through the subwavelength slits. The essential elements of the model, which describes a plasmonic damped wave with amplitude decreasing as the inverse of the film thickness [9], are represented in the sketch of Fig. 2(a). Basically, an incident monochromatic light beam with wave vector k_0 in air is linearly polarized perpendicular to the slit of subwavelength width w, milled in a metallic film with thickness t, and deposited on a dielectric substrate (BK7 glass).

The far-field intensity enhancement for the single slits involves multiple coupling processes [see Fig. 2(a)]. Initially, the incident laser light generates surface plasmons (SPs) on the metal film. Because of vertical plasmon coupling, which depends on the film depth, surface charges are induced on the top metal film and simultaneously a strong electric field is generated inside the slit. Subsequently, an SPP mode [18], i.e., an electromagnetic excitation propagating at the interface between the dielectric and the

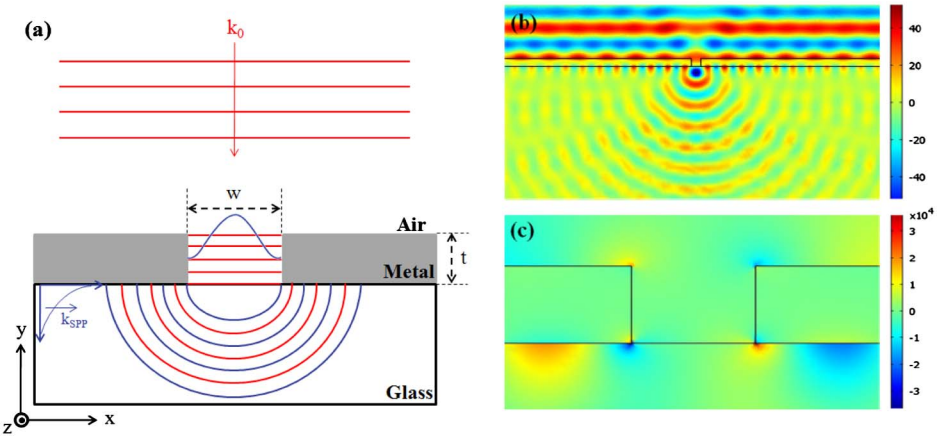

Fig. 2. (Color online) (a) Illustration of the adopted model. A single frequency incoming plane wave with wave vector k_0 in air is linearly polarized perpendicular to a slit of subwavelength width w, milled in a metallic film with thickness t deposited on a BK7 glass substrate. Here, k_{SPP} is the wave vector of the SPP mode. (b) and (c) 2D numerical simulations of a 150 nm slit fabricated in a 120 nm thick Ag film when illuminated by the line at 488.0 nm of an Ar ion laser, showing the amplitudes of the magnetic H field (along the z direction) and the electric E field (in the y direction), respectively. Length spans: (b) $x = 6\,\mu$m and $y = 3\,\mu$m, (c) $x = 0.3\,\mu$m and $y = 0.45\,\mu$m.

metallic conductor, evanescently confined in the perpendicular direction, is generated on the metal film/BK7 interface. This electromagnetic surface wave arises via the coupling of the electromagnetic fields to oscillations of the conductor's electron plasma. The SPP evanescent mode travels along the interface toward the slit, where it reconverts to a propagating wave and interferes with the traveling field directly transmitted through the slit. Additionally, penetration of the incident field inside the film enables the excitation of localized SP resonances [18] on the rim of the aperture, which contribute to the superposed output field. In this way, induced dipole moments at each rim form an "antenna coupling," which radiatively generate strong field enhancement (top and bottom). Then, the intensity of the resulting field can be written as

$$E \simeq \frac{E_i}{\pi}\frac{w}{t}\cos\left(k_{SPP}t + \frac{\pi}{2}\right), \qquad (1)$$

where $k_{SPP} = 2\pi/\lambda_{SPP}$, $\lambda_{SPP} = 2\pi/\mathrm{Re}[\beta]$, $\beta = k_0 n_{SPP}$, $n_{SPP} = (\varepsilon_{metal}\varepsilon_{glass}/\varepsilon_{metal} + \varepsilon_{glass})^{1/2}$, and $k_0 = 2\pi/\lambda_0$ [9,11,18]. Here, E_i represents the incoming plane wave in the y direction and λ_0 is its wavelength. Also, k_{SPP} and λ_{SPP} are the wave vector and wavelength of the SPP, β is the propagation constant of the superposed traveling wave, and n_{SPP} is the effective index of the SPP, which is for the interface between the metal and dielectric. In addition, ε_{metal} and ε_{glass} are the dielectric permittivities of metal and glass, respectively, and are functions of the excitation wavelength. In this sense, $\varepsilon_{Ag} = -7.89 + 0.74i$ and $\varepsilon_{glass} = 2.31$ are the tabulated dielectric constants of silver and BK7 glass in the wavelength of 488.0 nm. In the same way, $\varepsilon_{Au} = -9.49 + 1.23i$ and $\varepsilon_{glass} = 2.29$ are the corresponding dielectric constants of gold and BK7 in 632.8 nm [19]. Here it is important to point out that the wavelength values of 488.0 and 632.8 nm are known to be close to the plasmon excitation wavelength of silver and gold, respectively. Increasing the metallic film thickness leads to decoupling of the top and bottom antenna.

For illustration purposes, Figs. 2(b) and 2(c) show corresponding two-dimensional (2D) numerical simulations carried out with COMSOL Multiphysics for TM-polarized waves [20] of the magnetic H field (along the z direction) and electric E field (in the y direction) amplitudes, respectively, for a 150 nm slit fabricated in a 120 nm thick Ag film when illuminated by the line at 488.0 nm of an Ar ion laser. Figure 2(b) shows how the incident plane wave is modified by the existing subwavelength slit. It is possible to see that the considered wave is almost completely reflected from the unstructured part of the film. Around the slit entrance, the amplitude of the standing wave is markedly attenuated, where some lightwave transmission to the exit facet is apparent. On the dielectric/metal interface, a train of surface waves (SPPs) is evident together with waves propagating into space. In the rims, different charge configurations can be obtained, which can be symmetric or antisymmetrically coupled [21]. This coupling leads to determined charge configurations in each rim of the slit (top and bottom). From Fig. 2(c), these surface modes are clearly seen. It is possible to notice from the figure these relatively weak resonances (antisymmetrically coupled) on the facets of the slit associated with localized SPs, which are nonpropagating excitations due to direct light illumination of the conduction electrons of the metallic nanostructure coupled to the electromagnetic field [18]. A similar behavior was observed in the simulations for Au films when excited by the line at 632.8 nm of an HeNe laser. The main apparent difference is the lower transmitted intensity due to a higher absorption loss attributable to the particular characteristics of gold [19], i.e., $\mathrm{Re}[\varepsilon_{Au}] = -9.49$ in contrast to $\mathrm{Re}[\varepsilon_{Ag}] = -7.89$. This is verified in Fig. 3, where it can be seen that the normalized

transmission intensity for the Ag films is improved more than for the Au samples.

In general, the present numerical simulations qualitatively show appreciable light transmission through the slits. Actually, it was experimentally observed that the transmission sensitively depends on the metallic film thickness and slit width. As a first approximation, the theoretical slit transmission intensity can be given simply by the square modulus of Eq. (1). In this way, Fig. 3 plots as predicted [from Eq. (1)] and measured (using the setup shown in Fig. 1) transmission intensities as a function of the film thickness for the various slit widths milled in the Ag and Au samples. Also, the insets of Fig. 3 show the measured transmission versus slit width for certain film thicknesses. The relative slit transmission intensities are obtained by subtracting the background originating from the metal film and normalizing to the intensity from the wider slit structures. It is valuable to notice from Fig. 3 the very good correspondence between the theoretical estimate and the experiment. Therefore, taking into account the errors associated with the experimental determination of film thickness, slit width, and optical transmission intensities, it is possible to affirm that (1) the slits' transmission varies with metallic film thickness and presents a damped oscillatory behavior as the film thickness increases, and (2) the transmission increases linearly with increasing slit width for a fixed metallic film thickness. Although the general behavior is similar, distinct optical properties [19] lead to perceptible differences in the transmitted intensity and the position of maxima and minima between the Ag and Au films.

To help in elucidating the first observation, it is valuable to note that Fabry–Perot (FP) resonances are expected to contribute to the enhanced transmission of subwavelength slit arrays [4,5,16,22]. In this way, FP modes related to the finite depth of the slits in the present films should give rise to transmission maxima at certain wavelengths [22]. Actually, an accurate analysis recently published shows that the two maxima observed in Figs. 3(a) and 3(b) correspond to FP-like resonances within the slit volume for the first half-wave and full wave of the light within the slit [23]. In this sense, the FP multiple reflection effect within the slits leads to significant modulation of the transmission as a function of metal film thickness. These transmission maxima occur if the FP resonance condition is fulfilled [24]:

$$2k_0\mathrm{Re}\left[\frac{\lambda_0}{\lambda_{\mathrm{SPP}}}\right]t + \arg(\varphi_1\varphi_2) = 2m_y\pi, \qquad (2)$$

where m_y (the FP mode) is an integer and φ_1 and φ_2 denote the phase of the reflection coefficients of the slit at the incident and output interfaces, respectively. Thus, the effect of slit depth on the transmission enhancement can be easily understood. When the incident wavelength and slit depth are satisfied by Eq. (2), a transmission maximum will occur. Furthermore, from Eq. (2), it is expected that the transmission under a certain incident wavelength has a period of $\lambda_{\mathrm{SPP}}/2$ as a function of slit depth. The results of Fig. 3 can now be simply explained for the present Ag and Au films. Therefore, when the film thickness is near half- or full-integer wavelengths of the guided mode within the slit "cavity," optimal transmission is achieved, which implies a field enhancement inside the slit.

We can apply an FP analysis to obtain the finesse F from Fig. 3, given by

$$F = \frac{\pi}{2\sin^{-1}\left(1/\sqrt{f}\right)}, \qquad (3)$$

where $f = 4R(1-R)^{-2}$ is the finesse factor. Here, R is the reflectivity, given by $R = 1 - T$, where T is the

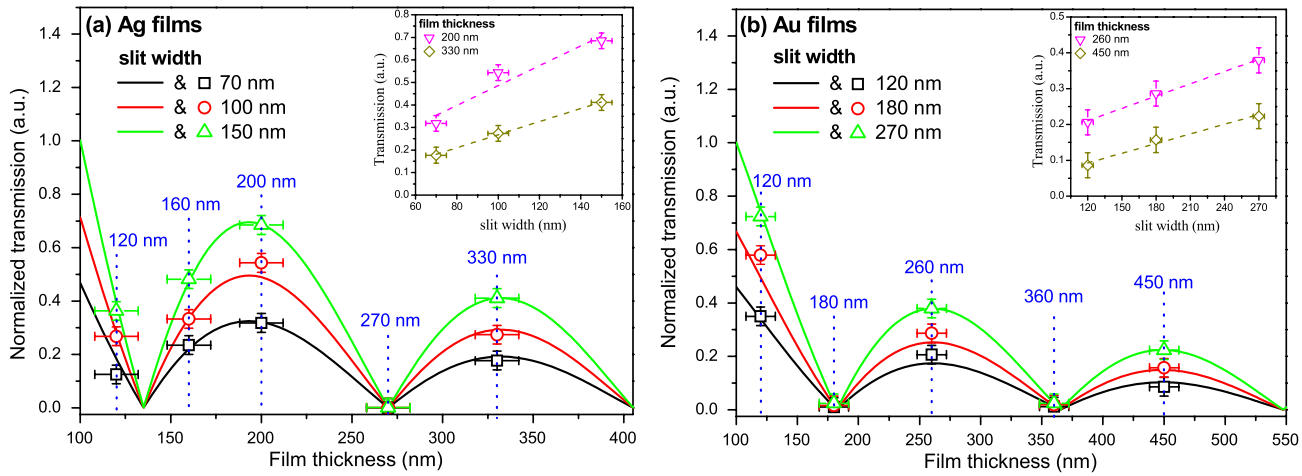

Fig. 3. (Color online) Theoretically estimated (lines) and experimental (symbols) normalized slit transmission intensities versus film thickness for the slits of the (a) 120, 160, 200, 270, and 330 nm thick Ag films, and the (b) 120, 180, 260, 360, and 450 nm thick Au samples. The dotted straight lines point out the thickness of the considered samples. In the minimum points, very low transmission values of the order of 10^{-2} were obtained. The insets show the measured transmission versus slit width for some film thicknesses. Here, the dashed straight lines are linear fittings of the experimental points.

transmission [25]. We determine from Fig. 3(a) for the Ag samples with 100 nm of slit width and thicknesses of 120, 160, 200, 270, and 330 nm, the reflectivities $R = 0.73$, 0.67, 0.46, 0.99, and 0.73, and the corresponding finesses $F = 9.98$, 7.74, 3.84, 312.58, and 9.89, respectively. From Fig. 3(b) for the Au samples with 120 nm of slit width and thicknesses of 120, 180, 260, 360, and 450 nm, we determine the reflectivities $R = 0.66$, 0.99, 0.79, 0.98, and 0.91, and the resultant finesses $F = 7.45$, 312.58, 13.27, 155.49, and 33.29, respectively. Here it is important to point out that for an FP cavity, the definition of quality factor (Q factor) is equivalent to the finesse [26]. Therefore, we can clearly see that both the R and Q factor values are significantly affected by the film thickness for a fixed slit width. Also, it is interesting to notice that near-zero transmission is a sign of high reflectivity values and high Q factors. For the maximum transmission points, a backward reasoning applies.

Finally, the fact that the transmission increases linearly with increasing slit width is in accordance with literature [27], where it was observed that the far-field transmitted intensity from a single slit shows a monotonic increase with the width, as expected from macroscopic intuition. In other words, the physical cavity length L_z and the optical cavity length $L_c(\lambda)$ are related, such that $L_c(\lambda) = L_z + 2\delta(\lambda)|r(\lambda)|^2$, where $r(\lambda) = |r(\lambda)| \exp(i\varphi)$ is the Fresnel coefficient, describes the shift of resonance wavelength from a perfect metal reflector due to field penetration $\delta(\lambda)$ into the metal mirror. But L_z is constant for all studied samples (20 μm), resulting in φ_z constant for a determined depth of metallic film. Nevertheless, the monotonic increase with the width w ($= L_x$) can also be explained considering FP resonances, for which we will use a simple analytical model to investigate the experimental results based on geometric arguments. Considering the standing wave mode in the cavity, when the penetration depth is ignored, the resonant condition of the slits can be written as

$$\frac{1}{{\lambda_{\mathrm{SPP}}}^2} = \left(\frac{m_z + \varphi_z}{2L_z}\right)^2 + \left(\frac{m_x + \varphi_x}{2L_x}\right)^2. \qquad (4)$$

We have applied Eq. (4) using the data of 200 nm of depth with widths $L_x = 70$, 100, and 150 nm for an Ag film, and 260 nm of depth with widths $L_x = 120$, 180, and 270 for an Au film. $L_z = 20\,\mu$m for both samples. Also, we considered in our calculations that φ_z and φ_x are practically constant, since we did not observe any peak shift in the transmission spectra of the samples in analysis. In the interface, values of $\lambda_{\mathrm{SPP\text{-}Ag}} = 269.9$ nm and $\lambda_{\mathrm{SPP\text{-}Au}} = 361.6$ nm were used. It was obtained for the Ag film $m_z = 78$ and $m_x = 1$, 1.4, and 2, and for the Au film $m_z = 145$ and $m_x = 1$, 1.5, and 2, i.e., an increase in L_x allows an increase in the transmission intensity spectra for a fixed depth [see insets of Figs. 3(a) and 3(b)].

4. Concluding Remarks

In summary, this work reports a systematic study of the optical transmission through slits with widths varied between 70 and 270 nm, fabricated with a focused gallium ion beam in Ag and Au samples possessing thicknesses in the range of 120–450 nm. A series of measurements of the far-field optical transmission through the slits has been undertaken. In addition, numerical simulations were performed. The simulations qualitatively reveal that the transmission profile is controlled by interference between the incident standing wave and plasmonic surface excitations. Quantitatively, a good correspondence between theoretical estimations and experiments was observed. It was possible to conclude that the slits' transmission is significantly affected by the metallic film thickness, presenting a damped oscillatory behavior as the film thickness is augmented. In addition, for a fixed metallic film thickness, the transmission increases linearly with increasing slit width. For a fixed wavelength and slit width, FP modes within the slits lead to significant modulation of the transmission as a function of metal film thickness. In this sense, film thickness and surface reflectivity are two important factors that can determine the interference pattern in FP-based devices. The appropriate control of such parameters, particularly the film thickness, can therefore maximize the performance of these devices.

The authors are indebted to Dr. M. A. Pereira-da-Silva (Instituto de Física de São Carlos, USP) for the atomic force microscopy measurements. This work was financially supported by the Brazilian agencies FAPESP and CNPq under CEPOF/INOF.

References

1. W. L. Barnes, A. Dereux, and T. W. Ebbesen, "Surface plasmon subwavelength optics," Nature **424**, 824–830 (2003).
2. E. Feigenbaum and H. A. Atwater, "Resonant guided wave networks," Phys. Rev. Lett. **104**, 147402 (2010).
3. T. W. Ebbesen, H. J. Lezec, H. F. Ghaemi, T. Thio, and P. A. Wolf, "Extraordinary optical transmission through subwavelength hole arrays," Nature **391**, 667–669 (1998).
4. J. A. Porto, F. J. Garcia-Vidal, and J. B. Pendry, "Transmission resonances on metallic gratings with very narrow slits," Phys. Rev. Lett. **83**, 2845–2848 (1999).
5. Y. Takakura, "Optical resonance in a narrow slit in a thick metallic screen," Phys. Rev. Lett. **86**, 5601–5603 (2001).
6. Y. Xie, A. R. Zakharian, J. V. Moloney, and M. Mansuripur, "Transmission of light through a periodic array of slits in a thick metallic film," Opt. Express **13**, 4485–4491 (2005).
7. H. J. Lezec and T. Thio, "Diffracted evanescent wave model for enhanced and suppressed optical transmission through subwavelength hole arrays," Opt. Express **12**, 3629–3651 (2004).
8. G. Gay, O. Alloschery, B. Viaris de Lesegno, J. Weiner, and H. J. Lezec, "Surface wave generation and propagation on metallic subwavelength structures measured by far-field interferometry," Phys. Rev. Lett. **96**, 213901 (2006).
9. G. Gay, O. Alloschery, B. Viaris de Lesegno, C. O'Dwyer, J. Weiner, and H. J. Lezec, "The optical response of nanostructured surfaces and the composite diffracted evanescent wave model," Nat. Phys. **2**, 262–267 (2006).

10. F. Kalkum, G. Gay, O. Alloschery, J. Weiner, H. J. Lezec, Y. Xie, and M. Mansuripur, "Surface-wave interferometry on single subwavelength slit-groove structures fabricated on gold films," Opt. Express **15**, 2613–2621 (2007).
11. D. Pacifici, H. J. Lezec, H. A. Atwater, and J. Weiner, "Quantitative determination of optical transmission through subwavelength slit arrays in Ag films: role of surface wave interference and local coupling between adjacent slits," Phys. Rev. B **77**, 115411 (2008).
12. E. Fontana, "Thickness optimization of metal films for the development of surface-plasmon-based sensors for nonabsorbing media," Appl. Opt. **45**, 7632–7642 (2006).
13. O. T. A. Janssen, H. P. Urbach, and G. W. Hooft, "On the phase of plasmons excited by slits in a metal film," Opt. Express **14**, 11823–11832 (2006).
14. X. Shou, A. Agrawal, and A. Nahata, "Role of metal film thickness on the enhanced transmission properties of a periodic array of subwavelength apertures," Opt. Express **13**, 9834–9840 (2005).
15. J. H. Kim and P. J. Moyer, "Thickness effects on the optical transmission characteristics of small hole arrays on thin gold films," Opt. Express **14**, 6595–6603 (2006).
16. Y. Pang, C. Genet, and T. W. Ebbesen, "Optical transmission through subwavelength slit apertures in metallic films," Opt. Commun. **280**, 10–15 (2007).
17. J.-Y. Laluet, A. Drezet, C. Genet, and T. W. Ebbesen, "Generation of surface plasmons at single subwavelength slits: from slit to ridge plasmon," New J. Phys. **10**, 105014 (2008).
18. S. A. Maier, *Plasmonics: Fundamentals and Applications* (Springer, 2007).
19. E. D. Palik, *Handbook of Optical Constants of Solids* (Academic, 1985).
20. Comsol Multiphysics, http://www.comsol.com.
21. E. Prodan, C. Radloff, N. J. Halas, and P. Nordlander, "A hybridization model for the plasmon response of complex nanostructures," Science **302**, 419–422 (2003).
22. F. J. Garcia-Vidal and L. Martin-Moreno, "Transmission and focusing of light in one-dimensional periodically nanostructured metals," Phys. Rev. B **66**, 155412 (2002).
23. J. Weiner, "The electromagnetics of light transmission through subwavelength slits in metallic films," Opt. Express **19**, 16139–16153 (2011).
24. Z.-B. Li, Y.-H. Yang, X.-T. Kong, W.-Y. Zhou, and J.-G. Tian, "Fabry–Perot resonance in slit and grooves to enhance the transmission through a single subwavelength slit," J. Opt. A **11**, 105002 (2009).
25. M. Born and E. Wolf, *Principles of Optics* (Pergamon, 1993).
26. L.-H. Shyu, C.-P. Chang, and Y.-C. Wang, "Influence of intensity loss in the cavity of a folded Fabry–Perot interferometer on interferometric signals," Rev. Sci. Instrum. **82**, 063103 (2011).
27. H. W. Kihm, K. G. Lee, D. S. Kima, J. H. Kang, and Q.-H. Park, "Control of surface plasmon generation efficiency by slit-width tuning," Appl. Phys. Lett. **92**, 051115 (2008).